ESTIMATION OF OBJECT LOCATION FROM SHORT PULSE SCATTER DATA

G.A. Tsihrintzis and A.J. Devaney

Dept. of Electrical and Computer Engineering
Northeastern University
Boston, MA 02115, USA

E. Heyman

Dept. of Electrical Engineering
Tel-Aviv University
Tel-Aviv, 69978, ISRAEL

ABSTRACT

We present an efficient algorithm for computation of the maximum likelihood estimate of the location of a known target from short pulse scatter data. The algorithm consitutes a three step procedure: (i) data filtering, (ii) time-domain backpropagation, and (iii) coherent summation and consists of a number of projection and backprojection operations integrated in a tomographic scheme. A computer simulation is included for illustration purposes and relevant applications in radar target identification and buried object detection are discussed.

Key words: Maximum Likelihood Estimation, Inverse Scattering, Tomography, Radon Transform, Target Recognition.

1. INTRODUCTION

In Inverse Scattering problems, an object (scatterer) is probed with wave pulses in an attempt to estimate (reconstruct) its structure from scattered radiation measurements [2]. In the present paper, we attempt to *detect* and *classify* a known target scatterer and *estimate* its location from limited and noisy *space-time* wave scatter data. The problem appears in application areas such as automatic radar target recognition, buried object detection and classification, and underwater fish population classification. We show that the maximum likelihood solution can be obtained via a computationally efficient algorithm in which the space-time measurements are first convolutionally filtered with the space-time target signature and subsequently tomographically backprojected.

The paper is organized as follows: Section 2 contains a review of the data measurement configuration, the wave scattering equations, and frequency-domain and time-domain plane-wave spectra of waves. Section 3 is concerned with location estimation algorithms and, after presentation of the frequency-domain solution, a time-domain filtered backpropagation algorithm is presented. Computer simulations are included is Section 4, while Section 5 contains a summary, a statement of conclusions, and a list of possible research avenues to be followed in the future.

2. CONFIGURATION AND SCATTERING EQUATIONS

A. Frequency-Domain Theory

Consider the data collection configuration in Fig. 1 in which known short plane-wave pulses illuminate a non-dispersive scattering object, characterized by the "object function" $O(\mathbf{r})$) and embedded in a dispersionless, non-attenuating homogeneous medium of wave velocity c_0. Let $\psi_0(\mathbf{r},t) = p(t - \frac{1}{c_0}\overset{\circ}{\kappa}\cdot\mathbf{r})$ be an incident plane-wave pulse propagating in the direction of the unit vector $\overset{\circ}{\kappa}$, where $p(\cdot)$ is a short pulse. The interaction of this pulse with the object results in the formation of a *scattered* wave pulse $\psi^s(\mathbf{r},t) = \frac{1}{2\pi}\int_{-\infty}^{\infty} d\omega\, e^{-i\omega t}\hat{\psi}(\mathbf{r},\omega)$ that is formally given as [5]

$$\hat{\psi}^s(\mathbf{r},\omega) = \int d^3r'\, k^2 O(\mathbf{r}')\hat{\psi}(\mathbf{r}',\omega)\hat{G}(\mathbf{r},\mathbf{r}',\omega). \qquad (1)$$

In Eq.(1), $\hat{\psi}(\mathbf{r}',\omega)$ is the temporal Fourier transform of the (measurable) *total* wave pulse, $\hat{G}(\mathbf{r},\mathbf{r}',\omega) = \frac{e^{ik|\mathbf{r}-\mathbf{r}'|}}{4\pi|\mathbf{r}-\mathbf{r}'|}$ is the frequency-domain Green function to the wave equation [5], and $k = \frac{\omega}{c_0}$ is the wavenumber in the background medium at temporal frequency ω.

Consider now an object function of the form

$$O(\mathbf{r};\mathbf{R}_c) = O_0(\mathbf{r}-\mathbf{R}_c), \qquad (2)$$

i.e., an object function O_0 that has been shifted in space by a vector $\mathbf{R}_c$. It was shown in [6] that the pulse scattered by the object $O_0(\mathbf{r}-\mathbf{R}_c)$ is related to the pulse scattered by the (centered) object $O_0(\mathbf{r})$ via:

$$\hat{\psi}^s(\mathbf{r},\omega;\mathbf{R}_c) = e^{ik\overset{\circ}{\kappa}\cdot\mathbf{R}_c}\hat{\psi}^s(\mathbf{r}-\mathbf{R}_c,\omega;0). \qquad (3)$$

B. Time-Domain Plane-Wave Spectra of Wavefields

Consider a time-domain wavefield $\psi(\mathbf{x},t)$ ($\mathbf{x} = x\,\overset{\circ}{x} + y\,\overset{\circ}{y}$), measured on the $z = 0$ plane, with equivalent frequency-domain representation

$$\hat{\psi}(\mathbf{x},\omega) = \int_{-\infty}^{\infty} dt\, e^{i\omega t}\psi(\mathbf{x},t). \qquad (4)$$

The frequency-domain plane-wave spectrum of the wavefield is defined as [5]

$$\hat{\tilde{\psi}}(\xi,\omega) = \int d^2x\, e^{-ik\xi\cdot\mathbf{x}}\hat{\psi}(\mathbf{x},\omega), \qquad (5)$$

where $k = \frac{\omega}{c_0}$ and ξ is a frequency-independent angular variable [5]. From Eq.(5), one can obtain the frequency-domain representation of the wavefield at an arbitrary point $\mathbf{r} = \mathbf{x} + z \overset{\circ}{z}$ in space as

$$\hat{\psi}(\mathbf{r}, \omega) = (\frac{k}{2\pi})^2 \int d^2 \xi e^{ik(\xi\cdot\mathbf{x}+\zeta z)} \tilde{\hat{\psi}}(\xi, \omega), \quad (6)$$

where $\zeta = \begin{cases} \sqrt{1-|\xi|^2}, & \text{if } |\xi| \leq 1 \\ i\sqrt{|\xi|^2-1}, & \text{else.} \end{cases}$ Eq.(6) is a result from the angular spectrum expansion of the frequency-domain causal (outgoing-wave) Green function to the Helmholtz operator [5] and clearly decomposes the wavefield $\hat{\psi}(\mathbf{r}, \omega)$ into a superposition of propagating (corresponding to $|\xi| \leq 1$) and evanescent (corresponding to $|\xi| > 1$) plane waves.

Eq.(5) has a time-domain equivalent, the time-domain plane-wave spectrum of the wavefield:

$$\tilde{\psi}(\xi, \tau) = \frac{1}{2\pi} \int d\omega \, e^{-i\omega t} \tilde{\hat{\psi}}(\xi, \omega). \quad (7)$$

Substitution of Eqs.(4) and (5) into Eq.(7) gives

$$\tilde{\psi}(\xi, \tau) = \int d^2\mathbf{x} \, \psi(\mathbf{x}, \tau + \frac{\xi\cdot\mathbf{x}}{c_0}), \quad (8)$$

as the time-domain relation between the wavefield and its plane-wave spectrum. Eq.(8) is recognized as a Radon transform [1] of the wavefield $\psi(\mathbf{x}, t)$ in the three-dimensional space $(\mathbf{x}, t)$ and has, thus, been termed a slant-stack transform [4]. Eq.(8) can be inverted to give the time-domain equivalent of Eq.(6). The inversion formula that includes the evanescent modes requires use of the analytic signal (see [3] for details). Here we will assume that the evanescent modes have been sufficiently attenuated to not contribute to the inversion formula. With this in mind, the result is

$$\psi(\mathbf{r}, t) = -\frac{1}{(2\pi c_0)^2} \int_{|\xi|\leq 1} d^2\xi \, \frac{\partial^2}{\partial \tau^2} \tilde{\psi}(\xi, \tau = t - \frac{\xi\cdot\mathbf{x}+\zeta z}{c_0}), \quad (9)$$

and can be recognized as a bank of inverse Radon transforms, each corresponding to a different z [1].

3. ESTIMATION OF OBJECT LOCATION

A. Data Model

Consider a scatterer described by the object function:

$$O(\mathbf{r}) = O_0(\mathbf{r} - \mathbf{R}_c), \quad (10)$$

where O_0 is a known function and $\mathbf{R}_c$ is an unknown scatterer location. The object is probed with short plane-wave pulses propagating in the direction of unit vectors $\overset{\circ}{\kappa}$, i.e., plane-wave pulses of the form $p_{\overset{\circ}{\kappa}}(t - \frac{\overset{\circ}{\kappa}\cdot\mathbf{r}}{c_0})$[1], and scattered pulse data are measured over planes perpendicular to the direction $\overset{\circ}{\kappa}$. We assume the measurement (data) model

$$y(\mathbf{r}_p, t, \overset{\circ}{\kappa}) \;=\; r_{\overset{\circ}{\kappa}}(\mathbf{r}_p, t) \otimes \psi^s_{\overset{\circ}{\kappa}}(\mathbf{r}_p + l\,\overset{\circ}{\kappa}, t; \mathbf{R}_c) + n_{\overset{\circ}{\kappa}}(\mathbf{r}_p, t) \quad (11)$$

$\mathbf{r}_p \in R^2, \quad -\infty < t < \infty, \overset{\circ}{\kappa}$ in some set of unit vectors, where $r_{\overset{\circ}{\kappa}}(\mathbf{r}_p, t)$ is a convolutional space-time measurement filter and $\psi^s_{\overset{\circ}{\kappa}}(\mathbf{r}_p, t; \mathbf{R}_c)$ is the scattered field. Additionally, $n_{\overset{\circ}{\kappa}}(\mathbf{r}_p, t)$ is zero-mean Gaussian noise, white[2] in the variables $\mathbf{r}_p$, t, and $\overset{\circ}{\kappa}$, i.e.,

$$\mathcal{E}\{n_{\overset{\circ}{\kappa}}(\mathbf{r}_p, t) n_{\overset{\circ}{\kappa}'}(\mathbf{r}'_p, t')\} = \sigma_n^2 \delta(\mathbf{r}_p - \mathbf{r}'_p)\delta(t-t')\delta_{\overset{\circ}{\kappa},\overset{\circ}{\kappa}'}. \quad (12)$$

The inverse problem is that of estimating the unknown parameter (object location) $\mathbf{R}_c$ from the measurements $y(\mathbf{r}_p, t, \overset{\circ}{\kappa})$ in Eq.(11).

B. Likelihood Function

We define

$$\alpha(\mathbf{r}_p, t, \overset{\circ}{\kappa}; \mathbf{r}_c) = r_{\overset{\circ}{\kappa}}(\mathbf{r}_p, t) \otimes \psi^s_{\overset{\circ}{\kappa}}(\mathbf{r}_p + l\,\overset{\circ}{\kappa}, t; \mathbf{r}_c) \quad (13)$$

to be the scattered pulse on the measurement plane (filtered by the measurement filter) for the object located at $\mathbf{r}_c$ and obtain an estimate $\hat{\mathbf{R}}_c$ of the unknown object location by maximizing with respect to a test object location $\mathbf{r}_c$ the likelihood function

$$\begin{aligned} L(\mathbf{r}_c) \;&=\; \sum_{\overset{\circ}{\kappa}} \int_{-\infty}^{\infty} dt \int d^2 r_p \, y(\mathbf{r}_p, t, \overset{\circ}{\kappa}) \alpha(\mathbf{r}_p, t, \overset{\circ}{\kappa}; \mathbf{r}_c) \\ &-\; \frac{1}{2} \sum_{\overset{\circ}{\kappa}} \int_{-\infty}^{\infty} dt \int d^2 r_p \, |\alpha(\mathbf{r}_p, t, \overset{\circ}{\kappa}; \mathbf{r}_c)|^2. \end{aligned} \quad (14)$$

Next, we further simplify the expression for the log likelihood function and obtain an algorithm that can be efficiently implemented on the computer.

Theorem 1 *If evanescent plane-wave spectra are ignored, the term* $\frac{1}{2}\sum_{\overset{\circ}{\kappa}} \int_{-\infty}^{\infty} dt \int d^2 r_p |\alpha(\mathbf{r}_p, t, \overset{\circ}{\kappa}; \mathbf{r}_c|^2$ *in the log likelihood function in Eq.(14) is constant with respect to* $\mathbf{r}_c$.

Theorem 2 *Ignoring evanescent plane-wave spectra, the term* $\sum_{\overset{\circ}{\kappa}} \int_{-\infty}^{\infty} dt \int d^2 r_p \, y(\mathbf{r}_p, t, \overset{\circ}{\kappa}) \alpha(\mathbf{r}_p, t, \overset{\circ}{\kappa}; \mathbf{r}_c)$ *in the log likelihood function in Eq.(14) is equal to*

$$-\frac{1}{(2\pi c_0)^2} \sum_{\overset{\circ}{\kappa}} \int_{|\xi|\leq 1} d^2\xi \, \frac{\partial^2}{\partial\tau^2} [\tilde{y}(\xi, \tau, \overset{\circ}{\kappa}) \bar{\tilde{\alpha}}(\xi, \tau, \overset{\circ}{\kappa}; 0)]|_{\tau = -\frac{\xi\cdot\mathbf{r}_{cp} + \zeta\overset{\circ}{\kappa}\cdot\mathbf{r}_c}{c_0}}, \quad (15)$$

where $\mathbf{r}_c = \mathbf{r}_{cp} + \overset{\circ}{\kappa} \cdot \mathbf{r}_c$.

Eq.(15) can be interpreted as follows: For each pulse, the scattered pulse data are Radon-transformed with respect to their space-time coordinates, filtered in Radon space, and inverse Radon-transformed (one inverse Radon transform per value of $\overset{\circ}{\kappa} \cdot \mathbf{r}_c$) into object space to form partial images of the log likelihood function. The Radon-space filter consists of the complex conjugate of the time-domain plane-wave spectra of the field scattered by the centered object $O_0(\mathbf{r})$. Finally, the partial images are coherently superimposed.

[1] The subscript $\overset{\circ}{\kappa}$ is used to indicate that the form of the pulses may, in general, be different from experiment to experiment.

[2] Gaussian noise of arbitrary color can be handled by expanding the algorithm of this section to include a proper whitening filter.

4. COMPUTER ILLUSTRATION

For simulation purposes, we consider a single scattering experiment in a two-dimensional geometry in which a target lies in the (x, z)-plane and is infinitely long and uniform along the y-axis. The probing pulse is incident from the direction of the positive z-axis and data are measured along the line $(x, z = l)$. The target signature (scattered pulse $\psi_0^s(\mathbf{r}, t)$ corresponding to the target located at the origin) is a pulse

$$\psi_0^s(\mathbf{r}, t) = \frac{\sigma^2}{c_0^2} \frac{q(t - \frac{|\mathbf{r}|}{c_0})}{\sqrt{|\mathbf{r}|}}, \quad \mathbf{r} = (x, z), \tag{16}$$

where σ^2 is the scatterer cross section and

$$q(t) = \begin{cases} \frac{2\beta}{T}[\cos(\beta t^2)[1 + 2\beta t^2] - 1], & \text{if } 0 < t < T \\ 0, & \text{else.} \end{cases} \tag{17}$$

Eq.(17) is the far field approximation to the field scattered by a point scatterer of cross section σ^2 when probed with an appropriate plane-wave pulse. The scattered field for arbitrarily located target is subsequently generated according to Eq.(3).

We assumed the scatterer to be located at the origin of the (x, z)-plane and chose the parameters $\sigma^2 = 1$, $c_0 = 1$, $\beta = 1$, $T = 1$, and $l = 5$. For the additive Gaussian noise, we examined three different cases with corresponding variances 0, 0.25, and 1. In Fig. 2, we show the scattered pulse at $(x = 0, z = 5)$ for time $0 < t < 16$ for the three noise levels. Finally, the likelihood functions computed via Eq.(15) are shown in Figs. 3 for the three noise levels.

5. SUMMARY, CONCLUSIONS, AND FUTURE WORK

In this paper, we established that the log likelihood function for estimation of the location of a target object from noisy short pulse scatter data can be computed via a time-domain, filtered backpropagation algorithm consisting of a sequence of direct and inverse Radon transforms of the space-time measurements. Target identification can also be performed via a similar algorithm, in which a bank is employed of filters matched to various target signatures. A computer simulation of a single scattering experiment was performed to illustrate the procedure, which revealed very high algorithm performance even in the case of very low signal-to-noise ratio. Further performance improvements can be achieved if multiple scattering experiments are utilized.

Related research issues to be addressed in the future include the derivation of proper location estimation algorithms for the cases of measurement planes that remain fixed from scattering experiment to experiment. This is the case in geophysical surveys in which the sensor array is fixed in space and several scattering experiments are performed, each with a different probing plane-wave pulse. Another avenue of future research seems to lead to the derivation of nonparametric algorithms for detection, location estimation, and classification of stochastic scattering objects. This problem appears in several underwater surveys. This and related research is currently pursued and its results will be announced shortly.

6. REFERENCES

[1] S. Deans. *The Radon Transform and Some of its Applications.* Wiley, New York, 1983.

[2] A. J. Devaney. Reconstructive tomography with diffracting wavefields. *Inverse Problems*, 2:161, 1986.

[3] T. Melamed. Phase-space beam summation: A local spectrum analysis of time-dependent radiation. *J. EM Waves Appl.*, 11:739–773, 1997.

[4] T. Melamed, Y. Ehrlich, and E. Heyman. Short-pulse inversion of inhomogeneous media: a time-domain diffraction tomography. *Inverse Problems*, 12:977–993, 1996.

[5] P. M. Morse and H. Feshbach. *Methods of Theoretical Physics, Parts I,II.* McGraw-Hill, New York, 1953.

[6] G. A. Tsihrintzis and A. J. Devaney. Maximum likelihood estimation of object location in diffraction tomography, Part II: Strongly scattering objects. *IEEE Trans. Signal Processing*, 39(6):1466, 1991.

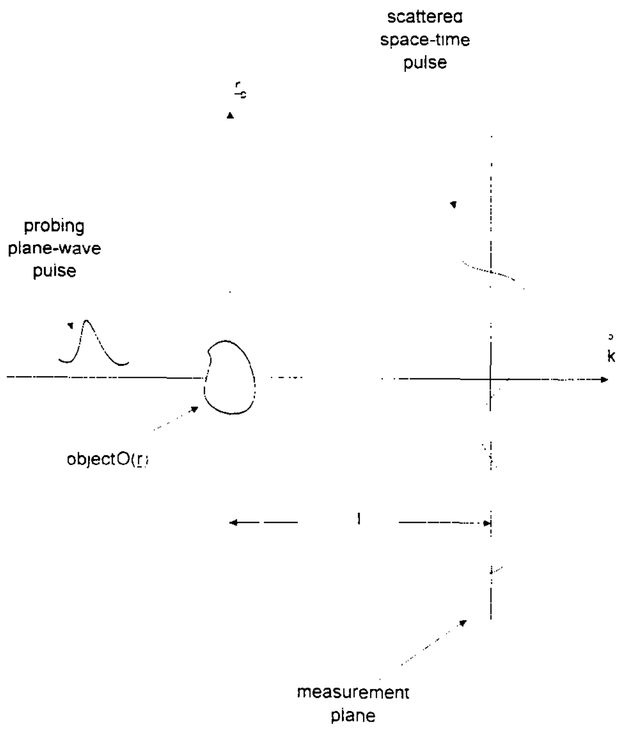

Fig. 1

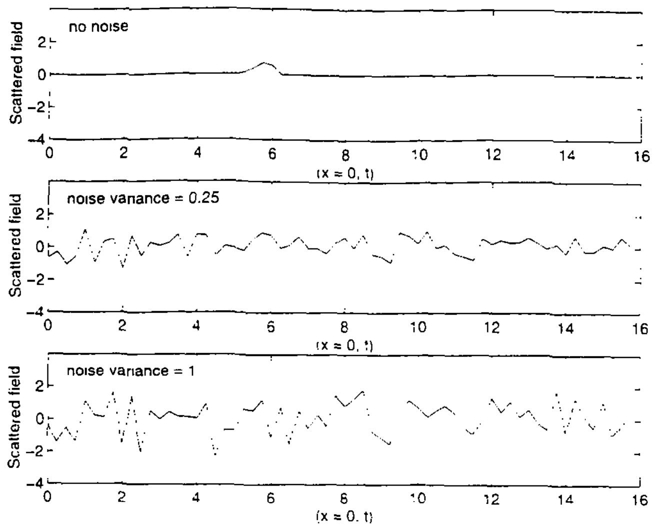

Fig. 2

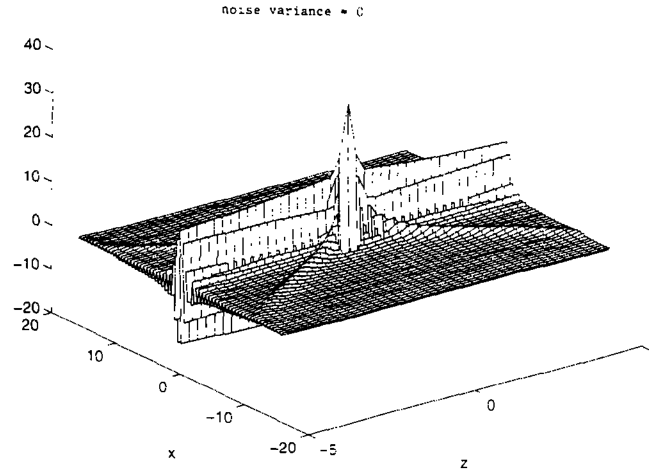

Fig. 3a

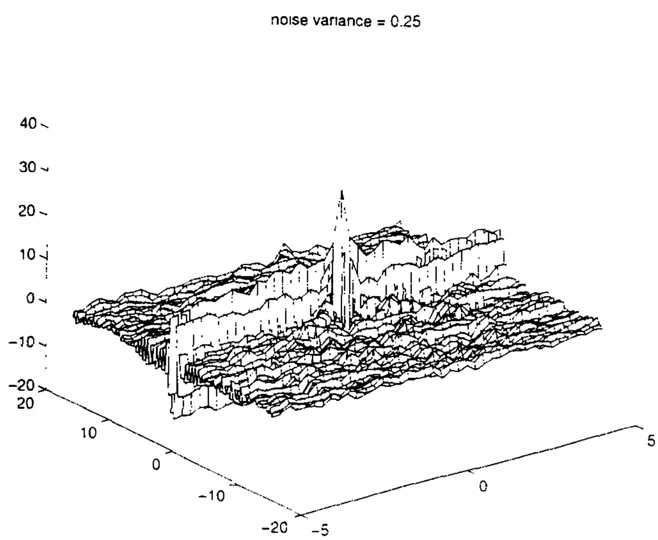

Fig. 3b

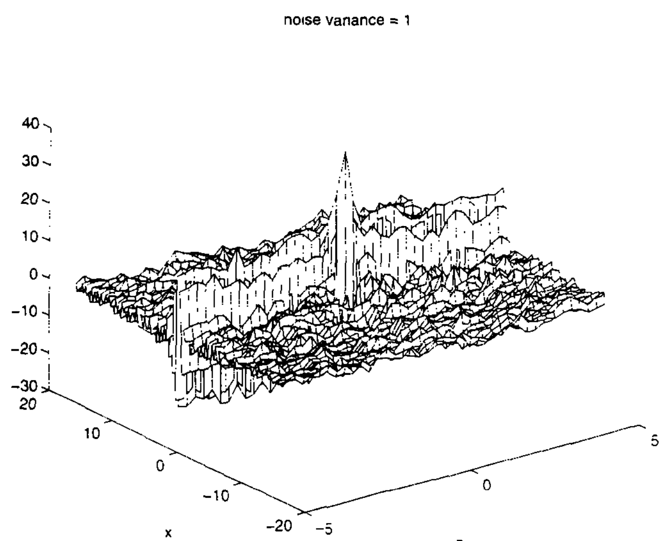

Fig. 3c